



SUBJECT AREAS:
GENES
TRANSCRIPTION
GENE REGULATION
GENETIC MODELS

Received
27 September 2011

Accepted
14 October 2011

Published
1 November 2011

Correspondence and requests for materials should be addressed to S.N.M. (smaity@mdanderson.org) or R.L. (Rong.luo@childrens.harvard.edu)

* Present address:
SNM Department of Genitourinary Medical Oncology, The University of Texas M.D. Anderson Cancer Center, 1515 Holcombe Blvd., Houston, TX; RL Division of Newborn Medicine, Department of Medicine, Children's Hospital and Harvard Medical School, 300 Longwood Avenue, Boston, MA

Inactivation of CBF/NF-Y in postnatal liver causes hepatocellular degeneration, lipid deposition, and endoplasmic reticulum stress

Rong Luo^{1,3*}, Sherry A. Klumpp², Milton J. Finegold⁴ & Sankar N. Maity^{1,3*}

From the Departments of ¹Molecular Genetics and, ²Veterinary Medicine and Surgery, The University of Texas, M. D. Anderson Cancer Center, ³Genes and Development Program, The University of Texas, Graduate School of Biomedical Sciences, ⁴Department of Pathology, Texas Children's Hospital, Houston, Texas 77030.

We previously demonstrated that CBF activity is needed for cell proliferation and early embryonic development. To examine the *in vivo* function of CBF in differentiated hepatocytes, we conditionally deleted *CBF-B* in hepatocytes after birth. Deletion of *CBF-B* resulted in progressive liver injury and severe hepatocellular degeneration 4 weeks after birth. Electron microscopic examination demonstrated pleiotropic changes of hepatocytes including enlarged cell and nuclear size, intracellular lipid deposition, disorganized endoplasmic reticulum, and mitochondrial abnormalities. Gene expression analyses showed that deletion of *CBF-B* activated expression of specific endoplasmic reticulum (ER) stress-regulated genes. Inactivation of *CBF-B* also inhibited expression of C/EBP alpha, an important transcription factor controlling various metabolic processes in adult hepatocytes. Altogether, our study reveals for the first time that CBF is a key transcription factor controlling ER function and metabolic processes in mature hepatocytes.

The endoplasmic reticulum (ER) stress pathway may play an important role in maintaining normal ER function and protecting hepatocytes from injury. A broad spectrum of insults to the liver, such as viral infections, metabolic disorders, and abuse of alcohol or drugs, can lead to ER stress^{1–3}. Induction of a distinct ER stress pathway occurs in the livers of diabetic mice, as well as in mice fed high fat diets and genetic models of obesity^{4,5}. While many studies have linked pathologic conditions of the liver with induction of ER stress, the factor(s) initiating activation of the ER stress pathway are unclear.

The ER stress pathway has evolved for cellular adaptation under various stress conditions such as increase in secretory protein synthesis, expression of misfolded proteins, glucose deprivation, perturbation in calcium homeostasis, and hypoxia. This pathway generally contains two major parts, 1) transcriptional stimulation of multiple chaperone genes to increase the protein-folding capacity of ER, and 2) general translational attenuation until normal ER function is restored. Prolonged ER stress can lead to cell death or various metabolic changes, including steatosis in liver^{6–8}.

Previously, analysis of ER stress-regulated promoters identified a composite promoter element, ERSE, that binds several different transcription factor such as CBF/NF-Y (CBF), ATF6, and XBP-1, which mediate transcription activation during ER stress^{9,10}. Among these transcription factors, CBF is constitutively expressed in mammalian cells, whereas both ATF6 and XBP-1 are activated by ER stress. CBF is needed for recruitment of ATF6 or XBP-1 to ERSE DNA, which then results in transcriptional activation of ER stress regulated genes^{11,12}. Knockout of XBP-1 in mice resulted in liver abnormalities, suggesting that the ER stress pathway could control normal liver development¹³. Interestingly, multiple CBF binding sites are found in the promoters of various ER stress-regulated chaperone genes such as GRP78, ERP72, and protein disulfide isomerase¹¹ that are needed for quality control of secretory proteins, suggesting that CBF may be essential for ER function in the liver under normal conditions.

Mammalian CBF consists of three subunits, CBF-A (NF-YB), CBF-B (NF-YA), and CBF-C (NF-YC), all of which are needed for DNA binding¹⁴. To understand the function of CBF *in vivo*, previously we utilized the gene-targeting method and Cre recombinase-loxP system to generate mouse strains harboring a conditional *CBF-B*

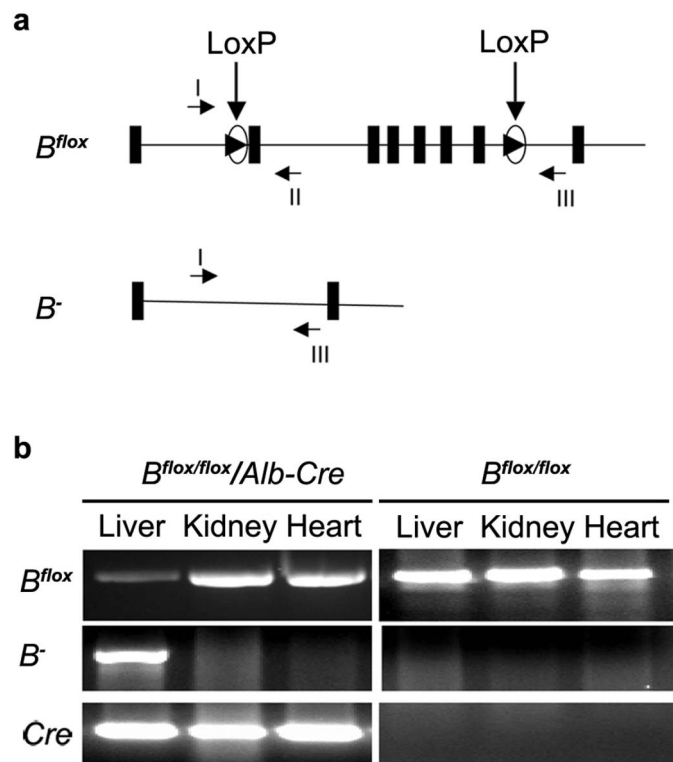


Figure 1 | Conditional deletion of floxed *CBF-B* (B^{flox}) allele in liver. (a) Intron/exon diagram of mouse B^{flox} and B^- alleles. Vertical thick bars and arrowheads within circle show relative locations of exons and loxP sites, respectively. Relative location for three primers, I, II and III, which were used for genotyping by PCR are shown by arrows. (b) Deletion of B^{flox} allele in liver of mice harboring *Alb-Cre* transgene. The DNA isolated from liver, kidney and heart tissues of various genotyped mice at 4 weeks after birth were amplified with primers I and II generating 250 bp DNA corresponding to B^{flox} allele, and with primers I and III generating 400 bp DNA corresponding to B^- allele. PCR with specific primers for cre recombinase gene generated 300 bp DNA.

allele, B^{flox} , containing one loxP site in intron 2 and one loxP site in intron 8 of the *CBF-B* gene, and a B^- allele containing a deletion from exon 3 to exon 8 of the *CBF-B* gene¹⁵. Heterozygous mice, with one B^{flox} and one B^- allele of *CBF-B*, were normal and fertile. However, no viable new-borns, and no embryos with homozygous $B^{-/-}$ allele were ever obtained in the crosses between the heterozygous mice. These results indicated that the *CBF* activity is required for early embryonic development and viability.

We speculate that *CBF* may affect ER function in hepatocytes in the mature liver. To test this possibility, the mice harboring the conditional *CBF-B* allele, B^{flox} , were mated with *Alb-Cre* mice harboring a transgene containing cre recombinase under the control of albumin promoter/enhancer¹⁶. The *Alb-Cre* mice express Cre

Table 2 | Percent death of *CBF-B* knockout mice between 4 and 6 weeks of age

Genotype	Total mice	Died at 4–6 weeks	% Death
Knockout $B^{flox/-}/Alb-Cre$	12	11	91.7%
$B^{flox/flox}/Alb-Cre$	12	4	33.3%
Control $B^{wt/flox}/Alb-Cre$, $B^{wt/-}/Alb-Cre$, $B^{flox/flox}$, and $B^{flox/-}$	41	0	0%

recombinase and induce deletion of the genomic locus flanked by loxP sites specifically in hepatocytes. This resulted in deletion of *CBF-B* gene postnatally exclusively in liver. Inactivation of *CBF-B* caused severe liver injury with progressive degeneration of hepatocytes, and induction of an aberrant ER stress pathway. Our study revealed that *CBF* is needed for expression of a subset of ER stress-regulated protein disulfide isomerase genes as well as the *C/EBP* alpha transcription factor in postnatal hepatocytes.

Results

Conditional inactivation of *CBF-B* in liver of newborn mice. To examine *CBF-B* deletion, 4-week old $B^{flox/flox}/Alb-Cre$ and $B^{flox/flox}$ mice were sacrificed to collect the liver, heart, and kidney for isolation of DNAs, which were used in PCR reactions to identify B^{flox} and B^- alleles. This showed that B^- allele was specifically generated in the liver but not in heart or kidney of $B^{flox/flox}/Alb-Cre$ mice, indicating that *CBF-B* gene was specifically deleted in liver (Fig. 1). Generation of the B^- allele was accompanied by reduction of B^{flox} allele in liver. The remaining B^{flox} allele in the liver indicated that recombination of loxP of *CBF-B* did not occur in every cell of the liver as described in a previous publication¹⁶. Quantitative PCR was done to measure B^{flox} and B^- alleles in tissue DNAs and showed that approximately 60% of the B^{flox} allele was deleted in the liver of both $B^{flox/-}/Alb-Cre$ and $B^{flox/flox}/Alb-Cre$ mice at 4 weeks of age (data not shown).

Inactivation of *CBF-B* in liver resulted in progressive liver injury.

To test hepatocyte viability, blood samples of mice at 4 weeks of age were examined for alanine aminotransferase (ALT) and aspartate aminotransferase (AST). ALT and AST were elevated in the blood of knockout mice compared to control mice (table 1). Total bilirubin was also increased in knockout mice. In contrast, both cholesterol and triglycerides were reduced, but creatinine concentration (a marker of kidney function) was not changed in knockout mice compared to control mice. These results indicated that the knockout mice were undergoing hepatocellular injury. When 12 $B^{flox/-}/Alb-Cre$, and 12 $B^{flox/flox}/Alb-Cre$ mice were monitored after 4 weeks of age, 11 $B^{flox/-}/Alb-Cre$ and 4 $B^{flox/flox}/Alb-Cre$ mice died between 4 and 6 weeks of age. In contrast, none of 41 littermate control mice died at this age (table 2). These results indicated that the postnatal deletion of *CBF-B* in liver is lethal in mice. The higher death rate in $B^{flox/-}/Alb-Cre$ line is likely due to a higher rate of *CBF-B* inactivation through a single *CBF-B* allele deletion, compared to

Table 1 | Analysis of blood serum of mice at 4 weeks age^a

Genotype	ALT	AST	Bilirubin	Cholesterol	Triglyceride	Creatinine
Knockout $B^{flox/-}/Alb-Cre$	341.00 ± 114.98	1528.67 ± 520.09	1.63 ± 0.40	57.11 ± 13.40	39.00 ± 9.89	ND
$B^{flox/flox}/Alb-Cre$	291.50 ± 149.20	1206.75 ± 382.30	0.50 ± 0.14	70.50 ± 4.90	64.00 ± 2.83	0.27 ± 0.028
Control $B^{wt/-}/Alb-Cre$	46.20 ± 11.50	183.17 ± 74.13	0.33 ± 0.12	124.50 ± 11.80	93.00 ± 2.82	0.28 ± 0.014
$B^{wt/flox}/Alb-Cre$						
$B^{flox/-}$						
$B^{flox/flox}$						

^aThe data presented for each component is the mean and standard deviations for independent measurements of blood samples from 7 $B^{flox/-}/Alb-Cre$ and 5 $B^{flox/flox}/Alb-Cre$ of knockout group, and 11 of control group mice. The standard deviations represented by error bars. The difference of ALT, AST, bilirubin, cholesterol, and triglycerides levels between the knockout and control group are significant ($P < 0.03$), whereas the difference of creatinine level is not significant. The creatinine level of $B^{flox/-}/Alb-Cre$ mice was not determined.



B^{flox/flox}/Alb-Cre line, which needs two CBF-B alleles to be deleted for CBF-B inactivation.

The livers of knockout mice at 4 weeks of age were pale and nodular compared to littermate control mice (Fig. 2 a–b). Histologic analysis at 2, 3, and 4 weeks revealed that the hepatocytes of knockout mice at 4 weeks were diffusely enlarged, as were their nuclei, and contained many microvacuoles within the cytoplasm (Fig. 2f) compare to the hepatocytes of controls at the same age (Fig. 2e). In addition, the livers of knockout mice displayed focal hepatocyte necrosis, mild lobular

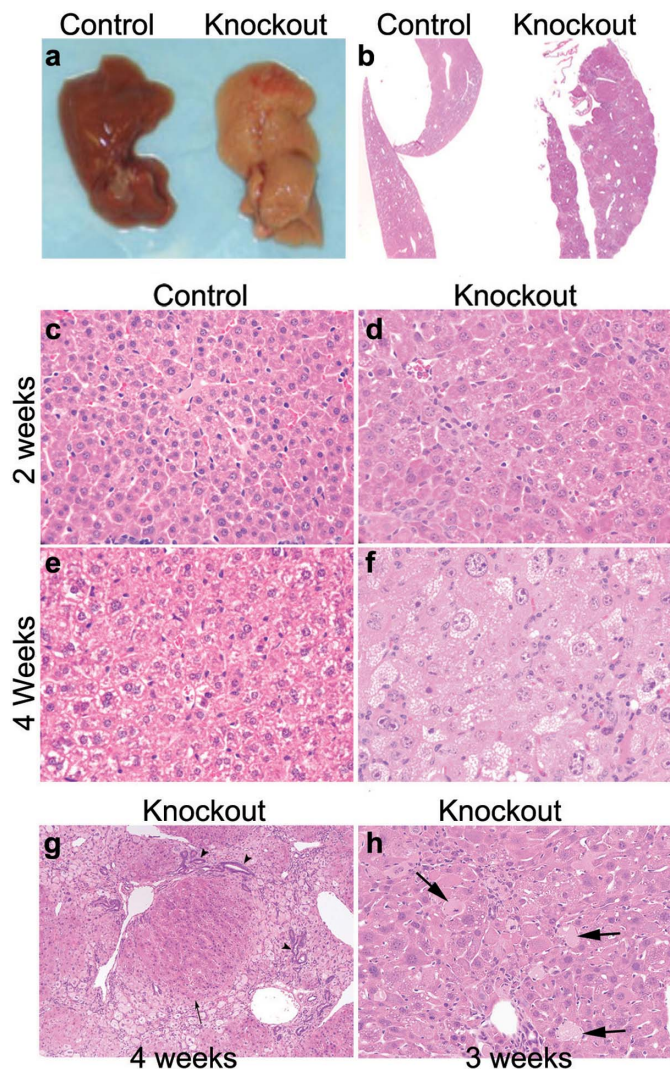


Figure 2 | Knockout of *CBF-B* results in hepatomegaly and liver steatosis. (a) Liver morphology of wild type and knockout mice. Photo shows livers from WT (left) and knockout mouse (right). The knockout livers had rough, pale to nearly white surface. (b) Histological analysis of liver sections from 4 weeks WT and knockout mice, (H&E stain, x12). (c–f) Hepatocellular injury after knockout of *CBF-B* at 2 and 4 weeks after birth, compared to wild type controls. The hepatocytes at 2 weeks are already larger than controls and their nuclei are also enlarged (upper panel). At 4 weeks, the hepatocytes of the control have grown but those of the knockout mouse are much larger with much larger and pleomorphic nuclei. They also contain numerous cytoplasmic vacuoles consistent with steatosis, and there are scattered small foci of hepatocellular necrosis and accompanying mid intralobular inflammation, (H&E stain, x400). (g) Livers of knockout mice at 4 weeks display focal bile ductular hyperplasia (arrowheads), and focal regenerative nodules (arrow), (H&E, x100). h, Arrows point to individual cell necrosis in 3 weeks CBF-B knockout livers. Cells are enlarged, have pale homogeneous cytoplasm and either a shrunken nucleus (upper left) or no apparent nucleus, (H&E, X200).

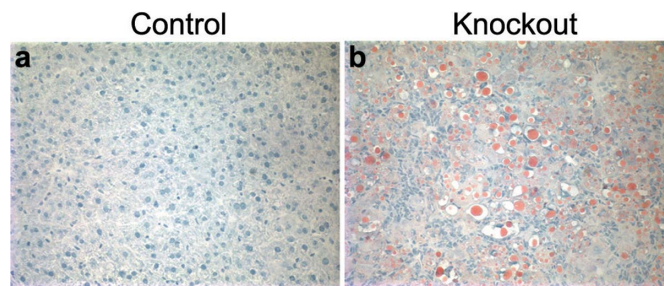


Figure 3 | Accumulation of fat in liver after knockout of *CBF-B* gene at 4 weeks. Frozen liver sections were stained with Oil red O, (x400). Significant lipid deposition was observed in knockout livers (right).

inflammation, increased numbers of sinusoidal cells, focal hyperplasia of bile ducts, and multiple regenerative nodules (Fig. 2g).

At 2 weeks age, the enlargement of hepatocytes was already evident in the knockout liver, but other changes in hepatocytes were less significant (Fig. 2d). By 3 weeks age, in addition to enlargement of hepatocytes, mild degenerative changes in hepatocytes including occasional necrotic and apoptotic cells were also observed in the knockout liver (Fig. 2h). Together, this analysis indicated that a progressive injury of the hepatocytes was due to the deletion of *CBF-B* gene after birth.

The sections of frozen liver tissue at 4 weeks of age stained with Oil Red O (ORO) showed that a large amount fat in the livers of knockout mice (Fig. 3). In contrast, no fat deposition was observed in the livers of control mice. Electron microscopy at 4 weeks age showed that the hepatocytes of knockout mice contained many lipid droplets, which accumulated in both cytosol and nucleus (Fig. 4b), and also displayed dilated smooth endoplasmic reticulum, and total depletion of glycogen (Fig. 4d). In addition, mitochondria displayed pleomorphism in the knockout hepatocytes compared to uniformity in control hepatocytes; additionally some mitochondria were elongated or circular or contained occasional paracrystalline arrays, none of which were observed in controls.

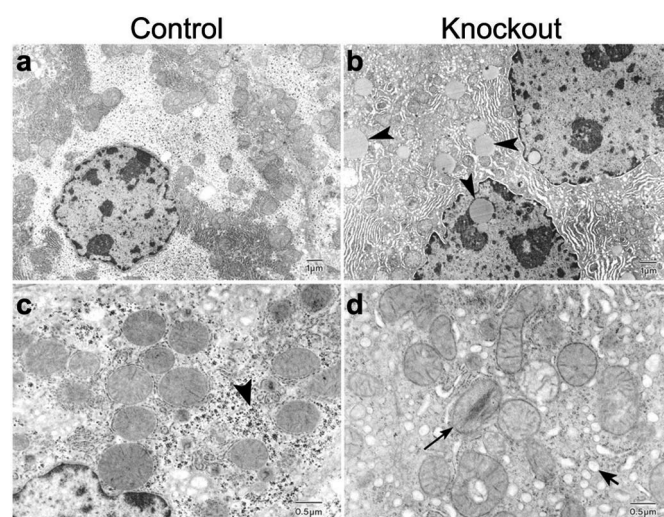


Figure 4 | Electron microscopy of hepatocytes after knockout of *CBF-B* gene, compared with controls at age of 4 weeks. Arrowheads in **b** panel indicate lipid droplets in knockout hepatocytes (x10,000). An arrowhead in **c** panel (x25,000) indicates normal abundance of glycogen rosettes in control hepatocytes, whereas none are found in the knockouts. The long arrow in **d** panel indicates an abnormal mitochondrion with a pseudocrystalline inclusion in knockout hepatocytes; other mitochondria in the figure display variation in size and shape. The short arrow in **d** panel indicates dilated smooth endoplasmic reticulum in knockout hepatocytes.



Inactivation of CBF-B resulted in altered expression of endoplasmic reticulum stress regulated genes. Based on previous promoter studies, we hypothesized that the loss of CBF activity could cause inhibition in expression of genes that are regulated during the cell cycle or during endoplasmic reticulum (ER) stress. To test this possibility, we isolated total RNA from livers of both control and knockout mice at 1, 2, 3, and 4 weeks of age after birth. Initially, we examined expression of XBP-1(s) and GADD153/CHOP (CHOP) for ER stress, cyclin B1 for cell cycle, and CBF-B to check for knockout efficiency. The XBP-1(s) mRNA, which is generated by splicing of XBP-1(u) mRNA as a result of IRE-1 kinase/endonuclease activation, was measured by RT-PCR (Fig. 5a).

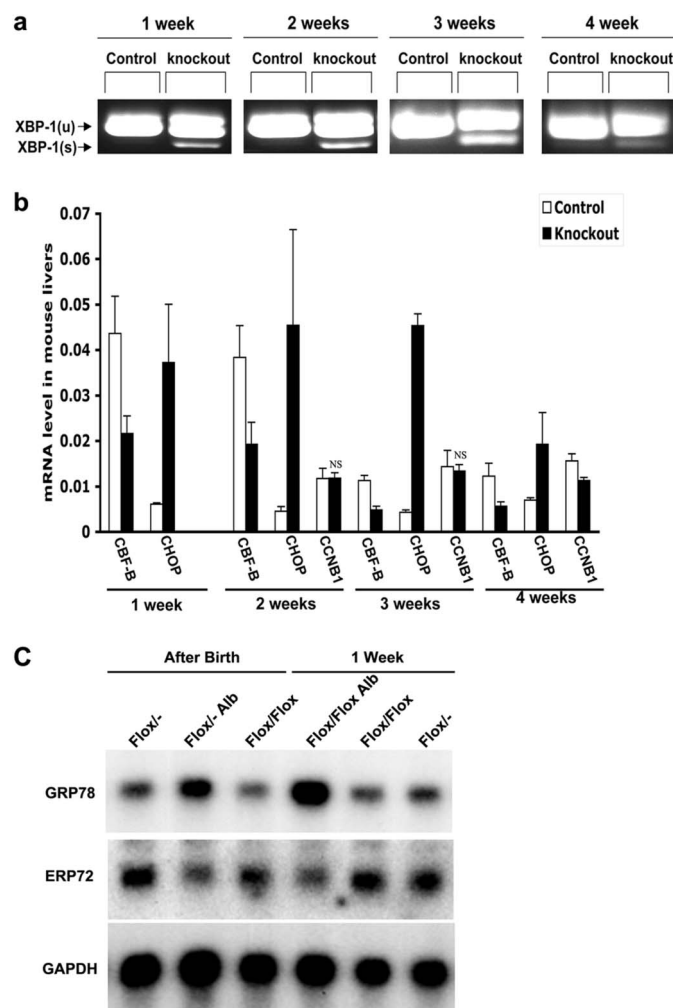


Figure 5 | Gene expression analysis in liver. (a) Analysis of XBP-1(s) expression in total liver RNA. Total RNAs were isolated from livers of both control and knockout mice at 1, 2, 3, and 4 weeks after birth, and were used in RT-PCR reactions to amplify both normal XBP-1(u) form of 246 bp, and spliced XBP-1(s) form of 220 bp in same reaction. (b) Analysis of expression of CBF-B, CHOP, and cyclin B1 (CCNB1) genes in total RNAs by quantitative RT-PCR method using SYBR green approach. Data presented in the histogram is the mean for 3 independent experiments using total RNAs from three different mice of each group at each time point. The standard deviations represented by error bars. The fold differences of CBF-B and CHOP between control and knockout mice at all tested time points are significant ($P < 0.008$). The fold difference of CCNB1 at 2 and 3 weeks is not significant (NS), but at 4 weeks is significant ($P < 0.02$). (c) Northern blot analysis of GRP78 and ERP72 gene expressions in livers of control and knockout mice after birth and at 1 week age. The GAPDH bands served as the RNA loading control.

Expression of CBF-B, CHOP, and cyclin B1 mRNAs was measured by quantitative RT-PCR (QRT-PCR) (Fig. 5b). Expression of both XBP-1(s) and CHOP was significantly activated in knockout but not in control livers at 1, 2, and 3 weeks, and modestly activated at 4 weeks of age. In contrast, expression of cyclin B1 was very similar between control and knockout mice, with a small reduction in liver of 4 weeks age knockout mice. This indicated that loss of CBF activity in liver specifically resulted in sustained activation of ER stress pathway from 1 week to 3 weeks, and continued at a modest level at 4 weeks after birth when significant pathology was observed. We then examined expression of several other genes that are also reported to be activated during ER stress. This demonstrated that loss of CBF activity also resulted in activation of expression of GRP78 in knockout livers at 2 and 3 weeks ages, but a slight reduction at 4 weeks age (table 3). In contrast, loss of CBF activity resulted in reduction of expression of three protein disulfide isomerase (PDI) family genes, ERP72, PDI and PDIA3, with a progressive reduction from 2 to 4 weeks. For example, expression of ERP72 was reduced by 9-fold at 4 weeks compare to 1.9-fold and 2.7-fold at 2 and 3 weeks. We also measured expression of C/EBP family and PPAR gamma transcription factors genes, which reflect the metabolic state of the liver^{17,18}. Expression of C/EBP alpha but not C/EBP beta was significantly reduced in the knockout livers at 2, 3, and 4 weeks of age (table 3). In contrast, expression of C/EBP delta and PPAR gamma was slightly increased in the knockout livers. To further confirm that ER stress induction is one of initial event after loss of CBF-B activity, we did gene expression analysis by northern blot after birth and at 1 week age. The expression of GRP78 and ERP72 dramatically changed just after birth (Fig. 5C), which suggested that ER stress is induced at early stage. Together, this analysis indicated that expression of PDI family and C/EBP alpha genes are dependent on CBF activity in postnatal liver.

Discussion

Our study demonstrates that deletion of CBF-B gene in liver resulted a progressive injury to hepatocytes, with significant changes in both cell and nuclear size, and other changes including focal necrosis, bile duct proliferation, and development of regenerative nodules at 4 weeks after birth of mice. Electron microscopy showed that inactivation of CBF-B resulted in multiple alterations of hepatocytes, which include intracellular and intranuclear lipid deposition, dilation of endoplasmic reticulum, mild pleomorphism of mitochondria, and marked depletion of glycogen. The endoplasmic reticulum became dilated in CBF-B knockout livers in response to the elevation of ER chaperone GRP78. This observation is consistent with previous finding¹⁹. Deposition of lipids in hepatocytes lacking CBF-B was also confirmed by Oil red O staining. Altogether, our study demonstrates that CBF-B, and thus CBF activity is essential for normal metabolic homeostasis of hepatocytes in vivo in mice after birth.

The gene expression analysis showed that deletion of CBF-B resulted in generation of XBP-1(s), and also stimulation of CHOP and GRP78 gene expression, all of which are usually activated by the unfolded protein response signaling pathway due to ER stress⁶. The inactivation of CBF, however, did not change expression of a cell cycle regulator, cyclin B1, which was found to be dependent on CBF in cultured cells in vitro²⁰. This indicated that CBF is specifically needed for ER function in hepatocytes. Further analysis in expression of other ER stress regulated genes showed that inactivation of CBF inhibited expression of ERP72, PDI, and PDIA3, which are members of protein disulfide isomerase (PDI) family that play role in oxidative protein folding. Thus, expression of ERP72, PDI, and PDIA3 is dependent on CBF activity in hepatocytes in vivo. A recent study demonstrated that inhibition of PDI activity induced ER stress and activated unfolded protein response in neuronal cells²¹; however no such study has been done in hepatocytes. We speculate that the inhibition in expression of the PDI family genes due to loss of CBF

Table 3 | Analysis of expression of different genes in total RNAs of control and knockout (KO) mice liver^a

Gene	2 weeks			3 weeks			4 weeks		
	Control	Knockout	Fold	Control	Knockout	Fold	Control	Knockout	Fold
GRP78	0.090 ± 0.0064	0.208 ± 0.025	+2.31	0.283 ± 0.020	0.683 ± 0.101	+2.41	0.669 ± 0.142	0.516 ± 0.0732	-1.30 (NS)
ERP72	0.088 ± 0.00078	0.046 ± 0.0072	-1.90	0.232 ± 0.0233	0.0853 ± 0.0112	-2.72	0.254 ± 0.0312	0.0281 ± 0.00724	-9.04
PDI	2.445 ± 0.095	1.823 ± 0.151	-1.34	0.595 ± 0.0585	0.341 ± 0.0421	-1.74	2.520 ± 0.256	0.760 ± 0.105	-3.32
Pdia3	0.683 ± 0.0404	0.597 ± 0.0556	-1.14	0.603 ± 0.0248	0.431 ± 0.0447	-1.40	1.268 ± 0.421	0.314 ± 0.0721	-4.04
C/EBP α	0.0143 ± 0.00455	0.00619 ± 0.00115	-2.31	0.0603 ± 0.00738	0.0275 ± 0.0115	-2.19	0.0619 ± 0.0330	0.00947 ± 0.00277	-6.54
C/EBP β	0.0423 ± 0.00476	0.0329 ± 0.00486	-1.28 (NS)	0.129 ± 0.0174	0.148 ± 0.0171	+1.14 (NS)	ND	ND	-
C/EBP δ	0.00329 ± 0.000226	0.00382 ± 0.000538	+1.16	0.00815 ± 0.000839	0.0112 ± 0.0023	+1.37	0.0102 ± 0.00180	0.0199 ± 0.00178	+1.95
PPAR γ	0.00963 ± 0.00106	0.0173 ± 0.00385	+1.80	0.0264 ± 0.00505	0.0460 ± 0.0112	+1.74	0.0164 ± 0.00761	0.0204 ± 0.00969	+1.24 (NS)

^aTotal RNA from 3 control and 3 knockout mice at each time point were used for the expression analysis by qPCR method. The data presented is the mean and standard deviations. Fold differences for C/EBPβ at 2 and 3 weeks, GRP78 and PPARγ at 4 weeks are statistically not significant ($P > 0.05$) as indicated by NS, whereas all the other fold differences are statistically significant ($P < 0.05$). Expression of C/EBPβ at 4 weeks was not determined.

activity caused an initial induction of ER stress and activation of unfolded protein response, which then stimulated expression of XBP-1(s), CHOP, and GRP78 genes.

Stimulation of GRP78 and CHOP after inactivation of CBF contradicted previous promoter studies that showed CBF binding to these promoters is needed for ER stress dependent transcription⁹. In this regard, ER stress results in activation of three transcription factors, ATF6(N), XBP-1(s) and ATF4, which then stimulate expression of genes encoding chaperones and folding enzymes⁶. Previous study demonstrated that CBF is required for DNA binding of ATF6 (N) and XBP-1(s) to ER stress elements present in various ER stress regulated genes^{10,22}. The XBP-1(s), however, also binds to the ER stress regulated promoters independent of CBF, and similarly, ATF4 binds to the ER stress promoters independent of CBF^{6,23}. These observations suggest that transcriptional activation during ER stress is partly dependent on CBF. Our analysis indicated that expression of PDI family genes is highly dependent on CBF under both basal and ER stress inducible conditions, and that expression of GRP78 and CHOP genes is activated through a CBF-independent mechanism.

Since activation of CHOP, GRP78, and XBP-1(s) was observed at 1 week after birth when no significant histological changes could be detected, induction of ER stress appears to be an early event in hepatocytes after inactivation of CBF. The transcriptional activation of ER stress genes is a part of cellular adaptive response to restore ER function. Because the PDI family genes could not be induced due to loss of CBF, there was an excessive and prolonged ER stress in hepatocytes observed by gene expression analysis. We believe that the prolonged ER stress is likely the major cause for pathological changes in hepatocytes after inactivation of CBF. Previous studies demonstrated that prolonged ER stress can result in cell death, which was activated by CHOP, and that it could also activate the SREBP transcription factor through translocation from ER to nucleus, resulting in activation of lipid biosynthesis genes and lipid deposition^{24,25}.

Our gene expression analysis also shows that inactivation of CBF significantly inhibited expression of C/EBP alpha but not C/EBP beta or C/EBP delta. Previous studies of C/EBP alpha gene ablation in mice demonstrated that C/EBP alpha is an important transcription factor that regulates several metabolic processes in hepatocytes during the perinatal period and also in adult liver²⁶. The postnatal deletion of C/EBP alpha resulted development of fatty liver and depletion of hepatic glycogen, as observed in our study after CBF-B deletion. This suggested that CBF might indirectly control metabolic processes in postnatal hepatocytes through regulating expression of C/EBP alpha.

Electron microscopy showed mild mitochondrial abnormalities after inactivation of CBF. Although our study does not provide any explanation for this change, it does suggest an interesting possibility that CBF also influences function of mitochondria in hepatocytes. In this regard, the HAP2, HAP3 and HAP5 genes, which are homologues of the CBF subunits in yeast, regulate mitochondrial oxidative phosphorylation in yeast¹⁴. The HAP complex in yeast controls the expression of several nuclear genes that play a role in mitochondrial oxidative phosphorylation. Thus it will be interesting to learn whether CBF controls any nuclear genes that function in mitochondria in hepatocytes in vivo.

In summary, our study demonstrates that CBF activity is needed for normal liver function after birth, and that it regulates expression of PDI family genes, and C/EBP alpha transcription factor, which play role in the function of endoplasmic reticulum, and metabolic processes.

Methods

Animals. The generation of B^{lox/lox} and B^{lox/-} mice maintained on a C57BL6 background has been described previously¹⁵. The *Alb-Cre* transgenic mice harboring a transgene containing Cre recombinase under control of an albumin enhancer/



promoter¹⁶, were obtained from the Jackson Laboratory (strain name- B6.Cg-Tg(Alb-cre)21Mgn/J), and were maintained as hemizygotes. The $B^{lox/+}$ mice bred with the Alb-Cre mice (homozygous for wild type CBF-B, B^{wt}) generated $B^{wt}/Alb-Cre$ mice (one wild type and one null CBF-B allele; hemizygous for Alb-Cre) or $B^{wt/lox}/Alb-Cre$ mice (one wild type and one floxed CBF-B allele; hemizygous for Alb-Cre). These mice were then mated with $B^{lox/+}$ mice to generate $B^{lox/+}/Alb-Cre$ and $B^{lox/lox}/Alb-Cre$ mice, which were used as knockout mice to examine the effects of CBF-B deletion in the liver. The littermates $B^{wt/lox}/Alb-Cre$, $B^{wt}/Alb-Cre$, $B^{lox/+}$, and $B^{lox/lox}$ were used as controls for each subsequent experiment. The mice were housed at the University of Texas M. D. Anderson Cancer Center animal facility according to the National Institutes of Health guidelines on the use of laboratory and experimental animals. All animal procedures are carried out as per the institutional guidelines for use of laboratory animals and as approved by the Ethics Committee of MDACC. Mice were given ad libitum access to food and water and underwent no treatment. Animals were euthanized at given time points, and the livers and other organs were quickly removed for various tissue preparations.

Serum analysis. Blood from 4-week old mice was collected by tail-vein bleeding in BD Microtainer Serum Separator Tubes. Serum was separated by high-speed centrifugation of the blood at 14,000 rpm for 2 minutes at room temperature. The serum samples were then assayed for aspartate aminotransferase (AST), alanine transaminase (ALT), bilirubin, cholesterol, and creatinine levels using COBAS INTEGRA 400 plus system (Roche), and the values were determined using a Hitachi 7170 automatic analyzer.

Histology. Liver specimens were fixed in 10% neutral buffered formalin, embedded in paraffin, sectioned at 5 microns and stained with hematoxylin and eosin. Hematoxylin and eosin stained slides were examined with a Leica DM 2500 microscope using 10×0.40 , 20×0.70 HC, and 40×0.85 HCX plan APO Leica objectives (Leica Microsystems, Bannockburn, Illinois). A Spot Insight 18.2 Color Mosaic camera (Diagnostic Instruments, Sterling Heights, Michigan) was used to acquire photomicrographs. Cell and nuclear measurements of hepatocytes were obtained with Spot software PC version 4.6.4.7 (Diagnostic Instruments, Sterling Heights, Michigan).

Electron Microscopy. 0.2 cm cubic portions of liver were immersed in 3% glutaraldehyde in 0.1 mol/L phosphate buffer, pH 7.4. After overnight fixation they were transferred to 0.1 mol/L phosphate buffer and then postfixed in 1% OsO₄ for 2 hours. The tissue was dehydrated in ethanol, rinsed in propylene oxide, and embedded in Epon. Sections (400 μm) were cut on a Reichert ultramicrotome, stained with uranyl acetate, and viewed and photographed in a JOEL 100CX transmission electron microscope.

Oil Red O Staining. Freshly dissected liver sections were embedded in OCT and snap frozen in liquid nitrogen. Cryostat sections cut at 6–7 microns were stained in a 0.3% solution of Oil Red O in 60% isopropanol for 1 h. After washing in 60% isopropanol, sections were counterstained with Gills hematoxylin. Sections were examined under bright-field microscopy with an Olympus model BX50 photomicroscope.

Extraction of RNA, Real-Time RT-PCR, and Northern Blot. Total RNA was extracted from livers at various time points after birth from both control and knockout mice (a minimum of 3 mice per group was used for each group at each time point) using an RNeasy mini kit (QIAGEN). Real-time RT-PCR was performed using the 1-step RT-PCR kit (Applied Biosystems, Foster City, CA) according to the manufacturer's instructions. Quantitative real-time RT-PCR was monitored using the ABI PRISM 7200 (Applied Biosystems), and the results were analyzed with the accompanying software. The SYBR Green PCR Master Mix (Applied Biosystems) was used for detection of mouse CBF-B, CHOP, cyclin B1, GRP78, ERP72, PDI, PDIA3, C/EBP alpha, C/EBP beta, C/EBP delta, and PPAR gamma. The S6, and beta actin were detected as internal controls to normalize the expression of the target genes. Primers for these PCR reactions were designed by using Primer Express 2.0 (Applied Biosystems, Rockville, MD), and the primer sequences are described in supplemental table S1. The XBP-1(u) and XBP-1(s) were detected by RT-PCR method using primers as described previously¹⁰. Ten micrograms of RNA from each sample was used for Northern blot analysis as previously described¹².

Statistical Analysis. All data were analyzed by paired student t-test, and were shown as means ± standard deviation. A P value of less than 0.05 was considered significant.

- Ji, C. & Kaplowitz, N. ER stress: can the liver cope? *J Hepatol* **45**, 321–333 (2006).
- Ji, C. & Kaplowitz, N. Hyperhomocysteinemia, endoplasmic reticulum stress, and alcoholic liver injury. *World J Gastroenterol* **10**, 1699–1708 (2004).
- Malhi, H. & Kaufman, R. J. Endoplasmic reticulum stress in liver disease. *J Hepatol* **54**, 795–809 (2011).
- Ozcan, U., et al. Endoplasmic reticulum stress links obesity, insulin action, and type 2 diabetes. *Science (New York, N.Y)* **306**, 457–461 (2004).
- McAlpine, C. S., Bowes, A. J. & Werstuck, G. H. Diabetes, hyperglycemia and accelerated atherosclerosis: evidence supporting a role for endoplasmic reticulum (ER) stress signaling. *Cardiovasc Hematol Disord Drug Targets* **10**, 151–157 (2010).

- Schroder, M. & Kaufman, R. J. The mammalian unfolded protein response. *Annu Rev Biochem* **74**, 739–789 (2005).
- van Anken, E. & Braakman, I. Endoplasmic reticulum stress and the making of a professional secretory cell. *Crit Rev Biochem Mol Biol* **40**, 269–283 (2005).
- Gentile, C. L., Frye, M. & Pagliassotti, M. J. Endoplasmic reticulum stress and the unfolded protein response in nonalcoholic fatty liver disease. *Antioxid Redox Signal* **15**, 505–521 (2011).
- Yoshida, H., et al. Endoplasmic reticulum stress-induced formation of transcription factor complex ERSF including NF-Y (CBF) and activating transcription factors 6alpha and 6beta that activates the mammalian unfolded protein response. *Mol Cell Biol* **21**, 1239–1248 (2001).
- Yoshida, H., Matsui, T., Yamamoto, A., Okada, T. & Mori, K. XBP1 mRNA is induced by ATF6 and spliced by IRE1 in response to ER stress to produce a highly active transcription factor. *Cell* **107**, 881–891 (2001).
- Roy, B. & Lee, A. S. The mammalian endoplasmic reticulum stress response element consists of an evolutionarily conserved tripartite structure and interacts with a novel stress-inducible complex. *Nucleic Acids Res* **27**, 1437–1443 (1999).
- Luo, R., Lu, J. F., Hu, Q. & Maity, S. N. CBF/NF-Y controls endoplasmic reticulum stress induced transcription through recruitment of both ATF6(N) and TBP. *J Cell Biochem* **104**, 1708–1723 (2008).
- Reimold, A. M., et al. An essential role in liver development for transcription factor XBP-1. *Genes & development* **14**, 152–157 (2000).
- Maity, S. N. & de Crombrugge, B. Role of the CCAAT-binding protein CBF/NF-Y in transcription. *Trends in biochemical sciences* **23**, 174–178 (1998).
- Bhattacharya, A., et al. The B subunit of the CCAAT box binding transcription factor complex (CBF/NF-Y) is essential for early mouse development and cell proliferation. *Cancer Res* **63**, 8167–8172 (2003).
- Postic, C. & Magnuson, M. A. DNA excision in liver by an albumin-Cre transgene occurs progressively with age. *Genesis* **26**, 149–150 (2000).
- Darlington, G. J., Wang, N. & Hanson, R. W. C/EBP alpha: a critical regulator of genes governing integrative metabolic processes. *Curr Opin Genet Dev* **5**, 565–570 (1995).
- Shi, X. L., et al. [Rapid simultaneous detection of Salmonella and Shigella using modified molecular beacons and real-time PCR]. *Zhonghua Liu Xing Bing Xue Za Zhi* **27**, 1053–1056 (2006).
- Goldshmidt, H., et al. Persistent ER stress induces the spliced leader RNA silencing pathway (SLS), leading to programmed cell death in Trypanosoma brucei. *PLoS Pathog* **6**, e1000731 (2010).
- Hu, Q., Lu, J. F., Luo, R., Sen, S. & Maity, S. N. Inhibition of CBF/NF-Y mediated transcription activation arrests cells at G2/M phase and suppresses expression of genes activated at G2/M phase of the cell cycle. *Nucleic Acids Res* **34**, 6272–6285 (2006).
- Uehara, T., et al. S-nitrosylated protein-disulphide isomerase links protein misfolding to neurodegeneration. *Nature* **441**, 513–517 (2006).
- Yoshida, H., et al. ATF6 activated by proteolysis binds in the presence of NF-Y (CBF) directly to the cis-acting element responsible for the mammalian unfolded protein response. *Mol Cell Biol* **20**, 6755–6767 (2000).
- Acosta-Alvear, D., et al. XBP1 controls diverse cell type- and condition-specific transcriptional regulatory networks. *Mol Cell* **27**, 53–66 (2007).
- Werstuck, G. H., et al. Homocysteine-induced endoplasmic reticulum stress causes dysregulation of the cholesterol and triglyceride biosynthetic pathways. *J Clin Invest* **107**, 1263–1273 (2001).
- Wu, J. & Kaufman, R. J. From acute ER stress to physiological roles of the Unfolded Protein Response. *Cell death and differentiation* **13**, 374–384 (2006).
- Yang, J., et al. Metabolic response of mice to a postnatal ablation of CCAAT/enhancer-binding protein alpha. *The Journal of biological chemistry* **280**, 38689–38699 (2005).

Acknowledgments

We thank Dr. Benoit de Crombrugge and Dr. Anuradha Bhattacharya for initial development of $B^{lox/+}$ mouse strain and also for many helpful discussions, James P. Barrish at Texas Children's Hospital Electron Microscopy Facility for EM preparation. This work was supported partly by a National Institutes of Health Grants RO1 AR46264 (to S. N. M.), a Living Legend Allocation for Molecular Genetics and Developmental Biology Priority Program, and an Institutional Research Grant from The University of Texas M. D. Anderson Cancer Center (to S. N. M.). The genotyping of mice were done by the DNA sequencing facility at The University of Texas M. D. Anderson Cancer Center, which is supported by a National Cancer Institute Grant CA 16672. Electron microscopy and ORO staining were done by the Texas Medical Center Digestive Diseases Center, which is supported by a National Institute of Diabetes and Digestive and Kidney Disease, Center Grant P30 DK56338

Author contributions

R.L. and S.N.M. jointly designed the experiments and analyzed data; S.N.M. supervised all biochemical and histological experiments and wrote the initial manuscript; R.L. carried out most experiments; S.A.K. did liver histology analysis; M.J.F. performed electron microscope analysis. All authors discussed the results and commented on the manuscript.



Additional information

Supplementary information accompanies this paper at <http://www.nature.com/scientificreports>

Competing financial interests: The authors declare no competing financial interests.

License: This work is licensed under a Creative Commons

Attribution-NonCommercial-ShareAlike 3.0 Unported License. To view a copy of this license, visit <http://creativecommons.org/licenses/by-nc-sa/3.0/>

How to cite this article: Luo, R., Klumpp, S.A., Finegold, M.J. & Maity, S.N. Inactivation of CBF/NF- κ B in postnatal liver causes hepatocellular degeneration, lipid deposition, and endoplasmic reticulum stress. *Sci. Rep.* 1, 136; DOI:10.1038/srep00136 (2011).